Esterification for biodiesel production with a phantom catalyst: bubble mediated reactive distillation.

William B Zimmerman[a] and Rungrote Kokoo[b]

[a]Department of Chemical and Biological Engineering, University of Sheffield, Mappin Street, Sheffield S1 3JD United Kingdom

[b]Department of Chemical Engineering, King Mongkut's University of Technology North Bangkok (KMUTNB), 1518 Pracharat 1 Road, Wongsawang, Bangsue, Bangkok 10800

Abstract

The initial aim of the paper is to dramatically improve the pretreatment stage of biodiesel production, which converts problematic free fatty acids to fatty acid methyl esters, by introduction of a microbubble mediated reactive distillation stage instead of acid pretreatment. This will shift the conventional esterification process towards completion with a yield higher than 80%, even without high excess methanol. Application of ozone microbubbles has the advantage over acid gas catalysis in that it gives higher conversion and leaves no catalyst residue and requires no further catalyst recovery separation steps (a "phantom" catalyst). Unreacted ozone breaks down into oxygen, so the off-gases are just a humid air stream that can be vented. Importantly, ozonolysis breaks carbon-carbon double bonds into aldehydes and carboxylic acids. Many ester species were found after contacting the feedstock with ozone-rich microbubbles, depending on the molecular structure of the alcohols for the ozonolysis of oleic acid with alcohols, i.e., methanol, ethanol, n-propanol, iso-propanol, and n-butanol. In the case of ozonolysis of used cooking oil mixed with methanol, the results from the GC-MS show that all saturated free fatty acids (including palmitic acid, stearic acid, and myristic acid) are converted to methyl esters within 20 hours of 60°C ozonolysis, whereas trace amounts of these chemicals remain at lower temperatures. The results also show that the conversion of oleic acid to form oleic acid methyl ester is 91.16% after 32 hours of ozonolysis at 60°C. Therefore, the free fatty acid content in used cooking oil is less than 1.33%, which makes it suitable as a reactant for biodiesel production via transesterification. However, this result is different from the result provided by ASTM D974 in that the acid numbers decrease dramatically by 25% at the beginning of ozonolysis followed by a plateau. Moreover, if the fluidic oscillator is used to generate bubbles in ozonolysis of oleic acid mixed with methanol, the results show that the yields of ozonolysis product 1-nonanal increase by 30%. This observation means that ozonolysis of oleic acid is relative to the specific interfacial area, and favoured at low liquid temperatures.

I. Introduction

Due to the increase of global energy consumption, limited fossil resources and environmental concerns, environmental technologies to produce energy from the renewable sources with low processing and capital cost are highly sought after. Biodiesel is a promising target for intensification and process improvements. Various methods for biodiesel production have been explored: homogeneous, heterogeneous, enzymate catalyzed and non-catalytic transesterification. Enzymatic catalyzed transesterification is found to be very expensive, while non-catalytic transesterification is carried out at high temperature, pressure with the requirement of high molar ratio of alcohol to oil [1-3]. Transesterification over alkali catalyst is, so far, the best method for biodiesel production [4] from various renewable feed stocks i.e., vegetable oils, animal fats and used cooking oils (UCO) [5]. The cost of UCO is two to three times less than that of pristine commodity vegetable oils, which leads to a significant reduction in the production cost [6]. However, the use of UCO, which contains significant levels of free fatty acids (FFAs) and water, over alkali catalyst has many serious drawbacks owing to soap formation. This causes the limiting of conversion and difficulty for glycerol separation [7]. To overcome these difficulties, esterification of UCO using acid catalysts is commonly applied for reducing FFA levels to lower than 3% which is a suitable value for transesterification in the later step [8].

Although several techniques are utilized to minimize the FFAs levels, most of them require high operating temperature, making the process less efficient and more complicated [4]. Consequently, esterification for biodiesel production via both homogeneous and heterogeneous acid catalyst are valid alternatives. The use of sulfuric acid has been reported that it worked well only within the FFAs range of 15-25%, 5% of catalyst loading and methanol-to-FFAs molar ratio of nearly 20:1 [9]. Biodiesel production from crude Jatropha oil (acid value of 17.2 mg KOH/g) using a novel magnetic carbonaceous acid shows high activity, stability and recoverability with over 90% yields [10]. Non-edible oil (Calophyllum inophyllum) with FFAs of 15% was selected as a feed stock for biodiesel production over sulphonated carbon catalyst and high conversion (99%) was achieved [11]. Moreover, as a result of a significant amount of oleic acid found in UCO [12], several studies are focused on esterification of that fatty acid. Esterification of oleic acid using 1-butyl-3-methyllimidazolium tetrachloroferrate ([BMIM][$FeCl_4$]) and zeolite Y prepared from kaolin as a catalyst was studied and found that the conversion was 83.4% and 85%, respectively [13, 14]. However, the quantitative conversion of 100% was observed by using picolinic acid modified 12-tungstophosphoric acid [15] and chlorosulfonic acid modified zirconia [16] as a catalyst.

As stated above, even though both homogeneous and heterogeneous acid catalyst can be used to convert FFA to methyl ester, all experiments have to be conducted with substantial excess methanol, high operating temperature and catalyst loading. With reference to the block diagram (Figure 1) of the conventional biodiesel production plant with acid esterification, pretreatment has a huge separation requirement. The vessels must be large and certainly must separate and recycle the excess methanol to be economically viable. The acid esterifier must separate the acid catalyst before transesterification, as transesterification uses alkaline catalyst for rapid kinetics, hence without removal of the acid catalyst, substantial salts and water will be unproductively formed. As it is, unreacted FFAs will form organic salts and water with some of the alkaline catalyst, requiring separation and additional alkaline provision to replace the spent catalyst incorporated in the salts. Although the aqueous phase (water, salts, glycerol and methanol) will phase separate from the FAME, the downstream separations require vacuum distillation for water and methanol removal and ion exchange resins to remove the salts and purify the glycerol [4]. All these processing steps are energy intensive.

The esterification pretreatment stage would improve the downstream separation efficiency dramatically if water were removed prior to transesterification. Zimmerman et al. [17] proposed a rapid evaporation methodology with hot, dry microbubbles, which vaporises water dramatically faster than hot, dry fine bubbles. Introducing dry fine bubbles, not even microbubbles, however, would strip the water from the reacting mixture. Conceptually, reactive distillation can achieve completion according to Le Chatelier's principle for equilibrium reactions. Removing the water would drive the reaction to competition as each molecule of water removed by vaporisation would be replaced by a molecule of water by further reaction. Unfortunately, injection of hot microbubbles alone into the acid esterification reactive mixture described by Talebian-Kiakalaieh et al. [4] with high excess methanol would not achieve the desired effect. Using acid catalysis, they varied controlling operation parameters such as methanol to oil ratio, catalyst loading, reaction temperature, and reaction time. Their evaluation gave highest conversion (88.6%) at the optimum condition of 70:1 methanol:oil, 65˚C temperature, 10 wt% catalyst, and 14 h reaction time.

Abdulrazzaq et al. [18] describe the strongly non-equilibrium preference for ethanol vaporisation in ethanol-water mixtures by hot microbubble injection. Subsequent modelling by Abdulrazzaq et al. [19] clarifies that the non-equilibrium driving force is kinetically much more rapid at vaporising ethanol in all liquid proportions. Since methanol is more volatile than ethanol, it would be expected to even more rapidly occupy the bubble vapor phase in contact with the esterification reacting mixture. So water will be removed, but methanol more preferentially. Since excess methanol is needed to push the

equilibrium in equation (1) while pulling it with water removal, hot bubble injection pulls the equilibrium but diminishes the push.

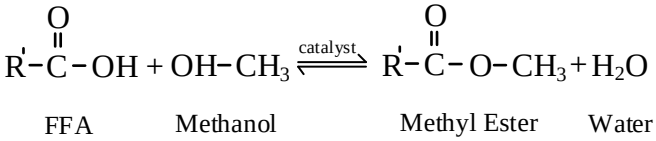

(1)

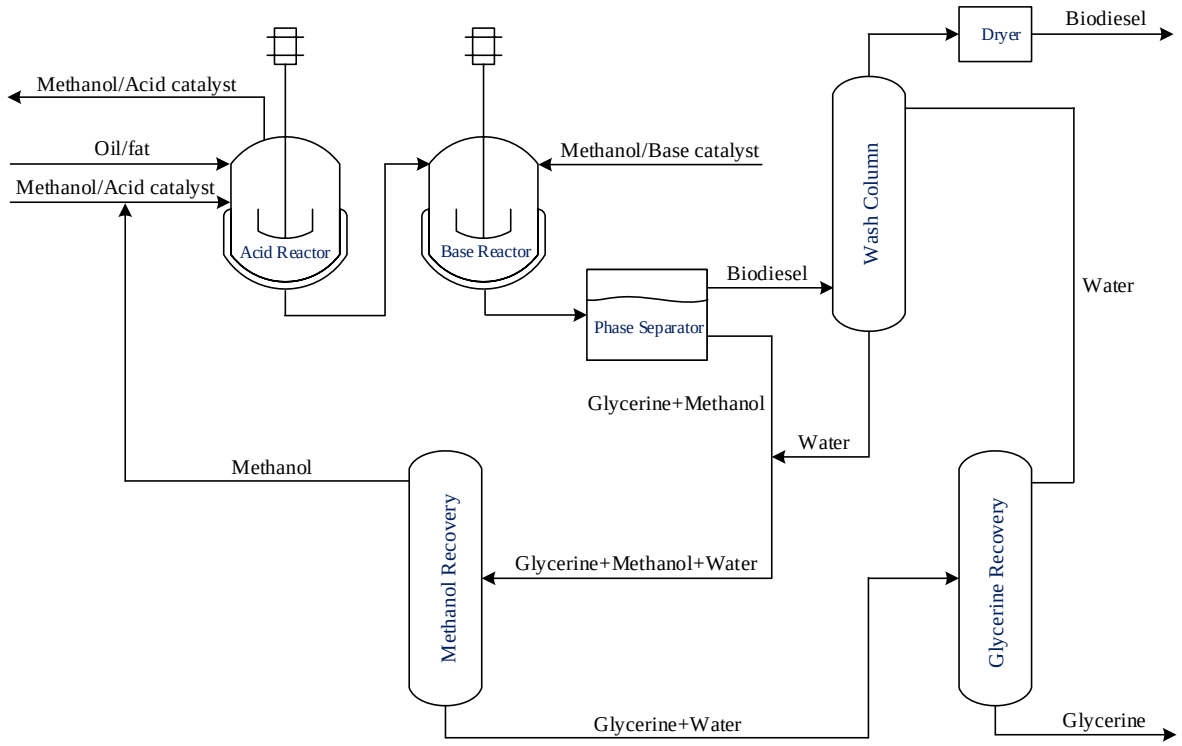

Figure 1 Conventional processing for high FFA bio-oils is a two-step process (modified from [20]). The first step is the acid reactor for esterification, which converts FFAs to FAME (biodiesel). The typical esterification is done with 20:1 excess methanol and sulphuric acid catalyst, but only achieves 60-80% conversion of the FFAs to biodiesel. The diagram shows the removal of the alcohol and acid catalyst from the acid reactor, which is a substantial separation step. The second step is the base reactor for transesterification. Unreacted FFAs from the first reactor will react with the base catalyst to form soap / salts. If above 4% FFA content, the glycerine, water and biodiesel will emulsify, destroying the product. Downstream separations are needed to recycle the methanol, remove salts and water from the glycerol, and water from the biodiesel.

Something more than just hot bubble injection is needed to overcome the propensity of methanol to vaporise. In this paper, we hypothesis that methanol that vaporises must become immediately reactive for bubble removal of water to be effective. The reaction should occur on the bubble interface, where water can join the dry bubble, and the methanol residue stays in the liquid phase as part of the methyl ester. To make the methanol reactive, we propose to form the methoxy free radical [21] whenever a methanol molecule enters the bubble. The bubble will be injected ozone-rich (see [22, 23]). Ozone is a free radical initiator, but actually it is possible to tune an in situ ozone plasma microreactor [24] so that oxygen singlet radicals are preferentially produced by selection of the residence time, and injected directly into the bubble. In the presence of water, oxygen radicals form hydroxyl radicals, but either

radical species will form water in the presence of methanol by scavenging the labile hydrogen from the alcohol group, forming the methoxy radical. The hypothesis suggested by this motivation is that ozone-rich bubbles injected into methanol-FFA mixtures (no acid or alkaline catalyst present) will be driven towards completion of esterification by the water removal mechanism, but catalysed by free radical chain reaction.

Although there are no claims in the literature that esterification can be free radical catalysed, Abdul-Majeed et al. [25] reported that the higher yield of FAME with injection of a flying plasma jet into used cooking oil than by the same source when treated by conventional transesterification This suggests that not only does plasma activation catalyse transesterification, but it catalyses esterification as well. Plasma jets, however, do not provide a route to vaporise water, so esterification would not be expected to go to completion if solely catalysed this way.

It should be noted that in competition with our hypothesis mechanism for ozone free radical initiated esterification is ozonolysis of the unsaturated carbon-carbon double bonds in the free fatty acid alkyl groups by the seminal mechanism proposed by Criegee [26]. Molecular ozone complexes with the carbon-carbon double bond (see Figure 2 for the case of oleic acid) which then breaks down into two pairs of Criegee intermediates (CIs), aldehydes and organic acids [27]. The organic acids, with lower molecular weight, can participate in esterification, leading to an overall lower average molecular weight fatty acid methyl ester – potentially less viscous than direct esterification of the unsaturated FAME without ozonolysis. The ozonolysis product aldehydes are valuable in their own right if separated, but may well be partially oxidised to organic acids in the presence of hydroxyl or oxygen free radicals. In this paper, we explore the competition between the known Criegee mechanism of ozonolysis and the hypothesized "phantom" catalysis of esterification.

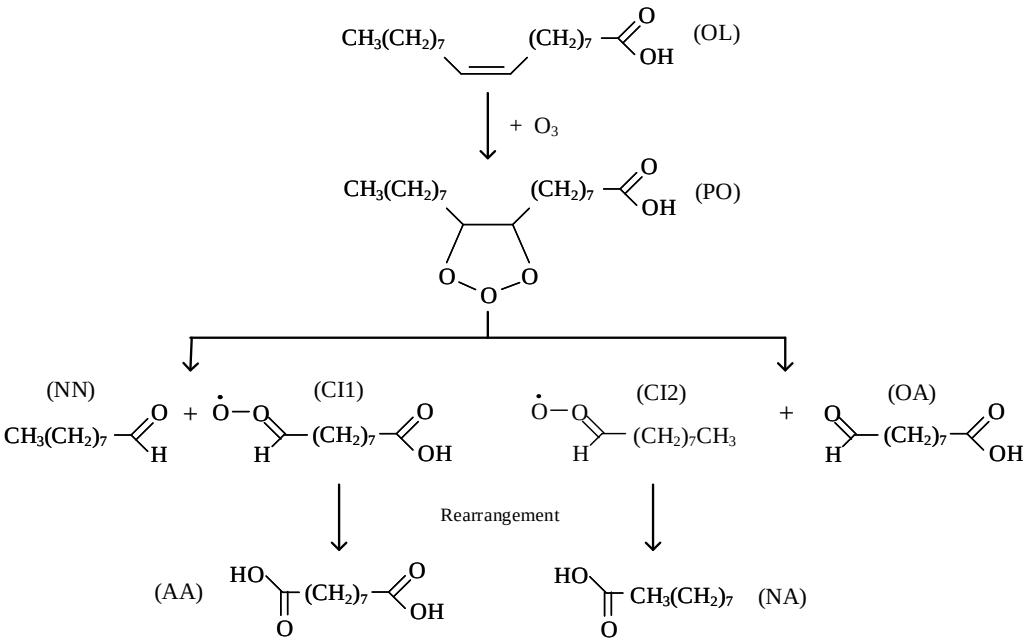

Figure 2: Possible ozonolysis products of oleic acid.

The major aim of this paper is to explore a hypothesis that forces esterification to completion, hence replacing the conventional acid reactor pretreatment for biodiesel production, which converts problematic FFAs to FAME, with a microbubble mediated reactive distillation stage. Microbubbles mediate esterification by providing a "phantom" catalyst and by removing the water product, thereby driving the reaction to completion via Le Chatelier's principle. The approach adopted here is to use

ozone as a free radical initiator for reaction on the bubble gas-liquid interface. The reaction vapor phase products, water and oxygen gas, are removed by the bubble. Hence the ozone vanishes after the reaction, but since it was generated from oxygen in situ, it is a reactive intermediate only.

This paper is organized as follows: Section 2 presents the materials and experimental methods for the ozonolysis of oleic acid and used cooking oil. Results and discussion are described in section 3, while in section 4 the summary and conclusion are drawn.

II. Methods and Materials

II. 1 Chemicals

Used cooking oil with different percentages of FFAs is used for ozonolysis instead of fresh vegetable oils because its price is 2.5 to 3.5 times cheaper than that of fresh vegetable oils of [4]. Methanol is also used as the solvent and reactant. Oleic acid (OL), the major component in olive oil, is a monounsaturated fatty acid that can react with ozone to form a number of valuable products, including 1-nonanal (NN), 9-oxononanoic acid (OA), nonanoic acid (NA), and azelaic acid (AA), as shown in Figure 2 [28]. Chemicals used in this paper were obtained from Sigma-Aldrich: oleic acid (99%), oleic acid (technical grade), 1-nonanal (95%), nonanoic acid (99.5%), azelaic acid (98%), acetone (HPLC grade), methanol (HPLC grade), ethanol (HPLC grade), n-propanol (99.5%), iso-propanol (99.5%), butanol (99.8%), methyl oleate (≥99%), methyl palmitate (≥99%), methyl nonanoate (≥99.8), methyl octanoate (99%), and sodium hydroxide (≥98%). Myristic acid (≥98%), Stearic acid (95%), Palmitic acid (≥98%), Toluene (HPLC grade, 99.9%), Alpha-Naphtholbenzein (indicator grade), Potassium hydroxide (reagent grade, >90%), and Barium hydroxide (technical grade, 95%) were obtained from Sigma-Aldrich.

II. 2 Used cooking oil preparation

Because used cooking oil contains a great amount of FFAs, and their composition must be the same in every experiment, the used cooking oil treated in this study was prepared by mixing pure olive oil with FFAs (20%). Synthesised used cooking oil should be colourless which is suitable for bubble characterisation. The compositions of FFAs (15.7%) in used cooking oil measured by Russbueldt and Hoelderich [12] are myristic acid (0.1%), palmitic acid (2.5%), palmitoleic acid (0.1%), stearic acid (1.2%), oleic acid (7.7%), linoleic acid (3.7%), and linolenic acid (0.4%). Therefore, four major FFAs, i.e., oleic acid, palmitic acid, stearic acid, and myristic acid, were selected to blend with olive oil for used cooking oil preparation; however, the compositions of oleic acid, palmitic acid, stearic acid, and myristic acid used in this study are slightly adapted to 75.8%, 16.5%, 7.6%, and 0.1%, respectively, and their details are listed in Table 1.

After the preparation process, used cooking oil was mixed with methanol for ozonolysis. It should be noted that the solution must exist as a single phase (homogeneous phase) after blending with methanol, and the minimum molar ratio of olive oil to methanol should be 1:3. To avoid two phases (heterogeneous phase), the ternary map of olive oil, OL and methanol was produced using Aspen Plus with UNIFAC-LL as the property method. This simulation result is quite similar to the experiment performed by Hirata et al. [29], who used canola oil instead. Two possible regions for the homogeneous phase were observed by fixing the percentages of FFAs in olive oil at 10%, 15%, and 20% and varying the molar ratio of olive oil to methanol. The first region is where the molar ratio of FFAs to methanol is low, whereas the second region is located where the molar ratio of FFAs to methanol is quite high. A low molar ratio between olive oil and methanol was selected in this study because the high molar ratio might not be possible in terms of economy.

Table 1 Chemical compositions of synthesised used cooking oil

Chemicals (wt.%)	**FFAs (wt.%)**		
	10	**15**	**20**

Olive oil	0.821	0.779	0.736
Oleic acid (OL)	0.068	0.103	0.139
Palmitic acid (PA)	0.015	0.023	0.031
Stearic acid (SA)	0.007	0.010	0.014
Myristic acid (MA)	576 ppm	875 ppm	0.001
Methanol	0.089	0.085	0.080

II. 3 Experimental set up

To generate bubbles, two techniques were used in this study, i.e., with and without the fluidic oscillator (FO). In case of FO use, dry air at 60 L/min, 20±1°C, and 15.1 psig was fed into the fluidic oscillator designed by Zimmerman et al. [30] to a generate pulse-jet stream. Dry air at only 0.1 L/min was fed into a plasma ozone generator (Adjustable OZ500 Ozone Generator, Dryden Aqua), and the remainder of dry air (59.9 L/min) was purged. However, without use of the FO, dry air at 0.1 L/min with the same temperature and pressure as those with use of the FO was directly fed into the plasma ozone generator, and the purge valve was closed.

After passing through the ozone generator, mixtures of ozone and dry air with the composition of 1600±50 ppm were fed into a glass bubble reactor with a diameter of 7.5 mm filled with a total of 325 ml of solvents. The inlet ozone concentration was measured using the iodometric method. The glass reactor was equipped with a diffuser with a diameter of 2.2 cm (ROBU Glasfilter-Gerate GmbH, Grade P4) made from borosilicate glass 3.3, a thermocouple, and a sampling tube. The heating mantle was connected to a temperature controller.

Because of volatile products that are possibly formed during the reaction, especially NN, a glass condenser with a surface area greater than 200 cm^2 was used to condense all volatile products and recycle them to the reactor using water as a cooling medium. The schematic of the experimental setup is shown in Figure 3. All tubing and connections were made of PTFE, glass or stainless steel for ozone resistance.

The experiments were conducted at 20±1°C, 40±1°C, and 60±1°C at atmospheric pressure. Samples of 1 mL were collected every 4 hrs for 36 hrs and stored in a refrigerator (< 4°C) prior to further analysis via GC-MS.

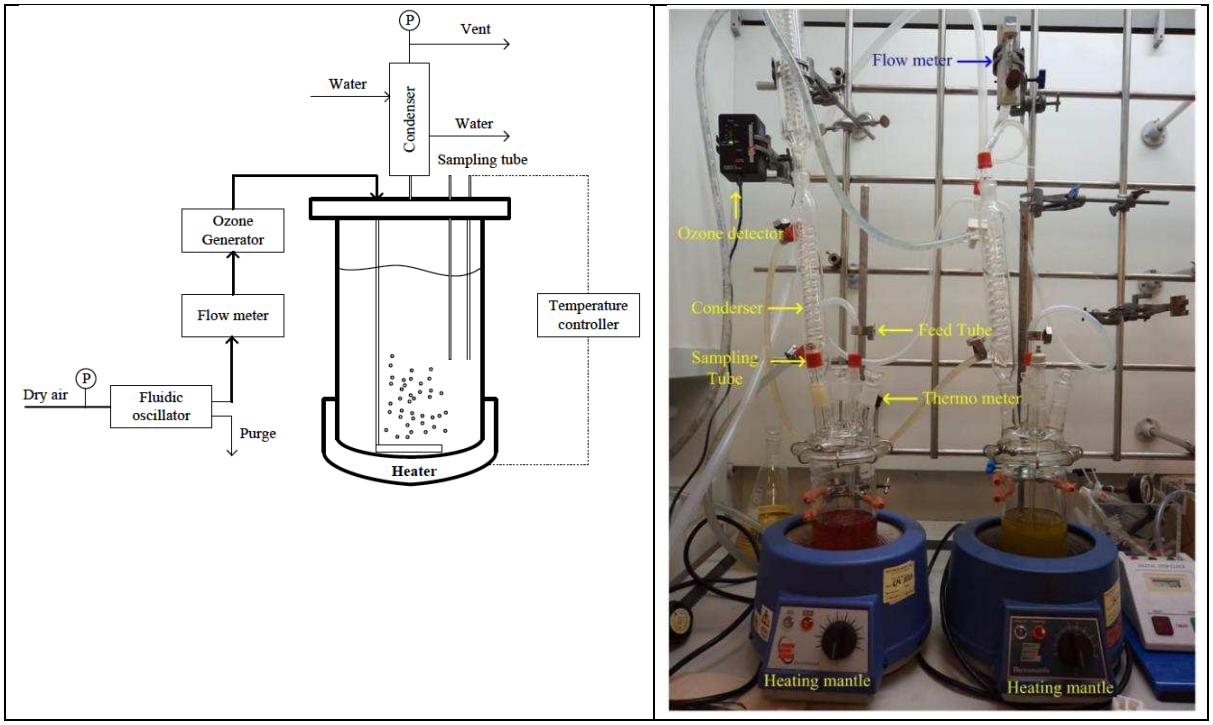

Figure 3 (left) Schematic diagram for an ozone microbubble injection into reactor chamber, with the vapours collected by cold water condensation for analysis. (right) Labelled picture of the bubble column reactors used in this study.

II. 4 Bubble size characterisation

The crucial parameter illustrating the kinetics of heterogeneous gas-liquid reactions by which ozone must transfer from gas phase to liquid phase simultaneously with reactions to other chemicals is the specific interfacial area. Measurement of the specific interfacial area poses the main difficulty in the kinetic study of the gas-liquid reactions, and this value is only obtained from experiments. In this work, a high-speed camera (Photron SA-3), which is able to capture 2000 frames/second, was used for bubble characterisation to determine the size distribution, gas holdup, and volume-surface mean bubble diameter. Halogen lamps (Model no: HM-682C: 150 W Argos, UK) were used as a light source. A constant of inlet flow and pressure must be set to control the bubble size. However, various bubble sizes were generated. The bubble size distribution must be, therefore, plotted to determine the mean diameter and the specific interfacial area. The experiment was performed in a clear glass reactor equipped with a sampling tube used as a referent scale as shown in Figure 3 (left). It should be noted that for accuracy in measurement, the size of the referent scale should be the same as that of the bubbles.

II. 5 GC-MS analysis

Samples of 10 µL were dissolved in 1 mL of acetone with a volume ratio of 1:100 before qualitative and quantitative analysis. The GC-MS used in these experiments is an HP 6890 series equipped with an HP 5973 mass selective detector and a HP1 19091Z-433 column, and helium was used as a carrier gas. The injection volume was set to 0.2 µL with an auto-sampler, and the pressure was set to 54 kPa. The temperature program was isothermal at 60°C for 2 minutes, increased at 10°C/min up to 300°C, and was held at 300°C for 6 minutes.

II. 6 Standard test method for acid number by colour indicator titration

In this study, the standard test method (ASTM D974) was used to determine the acid number of used cooking oil mixed with methanol after ozonolysis. This test method is commonly used to determine both acid and base numbers in petroleum products and lubricants that are soluble in the mixture of toluene, isopropyl alcohol, and water. This method can also be used for either new oils (light oils) or used oils (dark-coloured oil). All details can be found at the ASTM website (www.astm.org).

III. Results and discussion

III. 1 Bubble size characterisation

Bubble size always increases with decreasing liquid density as a result of low buoyancy force [31, 32]. However, in the case of vegetable oils and methanol solvents, the fluid viscosity exerts the main effect on the formation of the larger bubbles because the viscosity of, for instance, oleic acid (OL) is approximately 35 times higher than that of water. This observation is supported by Figure 4A, Figure 4C, and Figure 4E; the fluid density and surface tension of OL are quite similar to water except for the notably large difference in fluid viscosity. The fluid properties at different temperatures of 20°C, 40°C, and 60°C have been estimated by Aspen Plus. For example, the viscosities of OL at 20°C, 40°C, and 60°C are 35.26 cP, 18.17 cP, and 10.32 cP, respectively. According to these figures at different operating temperatures, the bubble size decreases with decreasing fluid viscosity. Moreover, the smaller size was observed when the system was operated with the fluidic oscillator, as shown in Figure 4B, Figure 4D, and Figure 4F, which is the same trend in the system operated without the fluidic oscillator in that the bubble size decreases with increasing temperature.

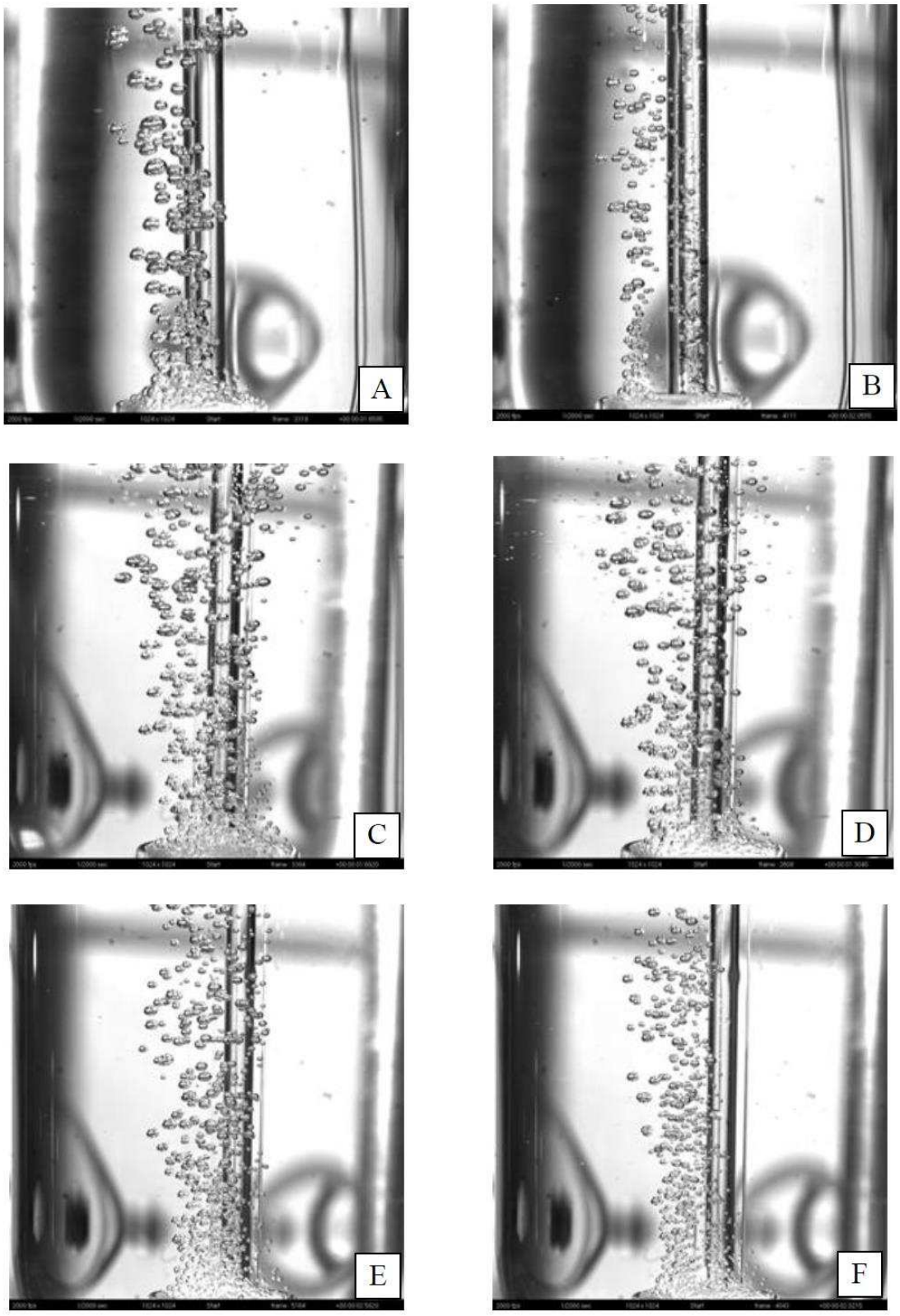

Figure 4 Images of the bubbles generated under OL with air flow 0.1 L/min; at 20ºC (A) without FO, (B) with FO, at 40ºC (C) without FO, (D) with FO, at 60ºC (E) without FO, (F) with FO

Table 2 Mean diameter and specific interfacial areas of the bubble phase at different temperatures at 0.1 L/min throughput for several oil solutions

Temperature (°C)	Mean diameter (µm)		Specific interfacial area (cm^{-1})	
	Without FO	With FO	Without FO	With FO
Pure OL				
20	1614	1000	0.0468	0.0709
40	1388	760	0.0513	0.0753
60	940	618	0.0734	0.1111
OL+ methanol				
20	1320	790	0.0504	0.0739
40	1077	734	0.0640	0.0920
60	818	491	0.0924	0.1350
Pure Olive oil				
20	2596	2149	0.0413	0.0595
40	2452	2082	0.0433	0.0642
60	1796	1296	0.0607	0.0892
Olive oil+ methanol				
20	2119	1647	0.0445	0.0652
40	1819	1304	0.0535	0.0763
60	1307	1007	0.0712	0.1028
Used Cooking oil+ methanol				
20	1936	1487	0.0460	0.0666
40	1666	1248	0.0572	0.0832
60	1166	916	0.0775	0.1128

After collecting photographs of the bubbles in the bubble column using the high-speed camera and analysis with ImageJ software (see [33]), the bubble size distribution with and without the fluidic oscillator at an air flow of 0.1 L/min was plotted at 20°C, 40°C, and 60°C, for pure OL and OL mixed with methanol, pure olive oil and olive oil mixed with methanol, and used cooking oil mixed with methanol, respectively. More than 500 bubbles were measured for reliable results [34]. The results show that the bubble size distribution without the FO appears as a normal size distribution, which is bell-shaped and symmetrically shaped, whereas the bubble size distribution with the FO appears as a left-skewed distribution. The narrower size distribution is also observed using the FO. This characteristic of the FO can be described using the log-normal size distribution, according to the experiment performed by Hanotu et al. [35]. Only the mean bubble diameters and specific interfacial areas of the bubble phase for these studies are reported in Table 2.

In addition to the difference in size distribution, at the same temperature, the bubble size of the system operated with the FO is smaller than that of the system operated without the FO as a result of the pulse-jet stream [36]. Bubble size generally increases with decreasing buoyant force, which is primarily a function of liquid density. Although, in this experiment, the density of OL decreases slightly with

increasing fluid temperature and results in the formation of larger bubbles, the observed bubble size decreases with increasing fluid temperature because of a sharp reduction in fluid viscosity [31, 32].

III.2 Ozonolysis of OL and alcohol

The formation of higher molecular weight products (HMWPs) that cannot be detected by GC-MS results in a loss of OL. Although certain lower molecular weight products (i.e., NN, OA, OcA, and hexanoic acid) are formed to increase productivity, the reaction must be performed at high temperature for higher molecular weight product decomposition. To increase the productivity at low temperature, short-chain alcohols are mixed with OL before starting the reaction. The chromatograms of OL ozonolysis at 20°C for 32 hours with methanol, ethanol, n-propanol, iso-propanol, and n-butanol are shown in Figure 5A, Figure 5B, Figure 5C, Figure 5D, and Figure 5E, respectively. It is interesting to note that not only NN but also many ester species are found after the reaction, depending on the molecular structure of the alcohols. For example, mixing with methanol produces NN, octanoic acid, methyl ester (M-Oc), nonanoic acid, methyl ester (M-NA), nonanal dimethyl acetal (DM-NN), 9-oxononanoic acid, methyl ester (M-OA), azelaic acid, methyl ester (M-AA), 2-Octanol, 8, 8-dimethoxy (DM-2Oc), palmitic acid, methyl ester (M-PA), and margaric acid, and methyl ester (M-HA). Both NN and DM-NN are considered to be major products and can be used as flavouring and fragrance agents in the perfume and food industries [37].

In addition to methanol, ozonolysis of ethanol and OL is studied under the same conditions as with methanol, and production of NN, octanoic acid, ethyl ester (E-OcA,), nonanoic acid, ethyl ester (E-NA), nonanal diethyl acetal (DM-NN), 9-oxononanoic acid, ethyl ester (E-OA), azelaic acid, ethyl ester (E-AA), 2-Octanol, nonane, 1, 1-diethoxy (DE-NN), palmitic acid, ethyl ester (E-PA), and margaric acid, and ethyl ester (E-HA) is observed. The formation of propyl ester, isopropyl ester and butyl ester (all carboxylic acids) are also observed by ozonolysis with n-propanol, iso-propanol or n-butanol, respectively.

According to the chromatograms shown in Figure 5, the greatest amount of NN is produced by ozonolysis of OL with methanol, and the remainder represents a slightly greater amount compared with that of pure OL ozonolysis. No sign of OA, which was observed at 20°C for 32 hours of reaction, is detected in mixing with alcohols because OA reacts with alcohols to form alkyl esters. All of the carboxylic acids found during ozonolysis of OL and FFAs (palmitic acid and heptadecanoic acid) also react with alcohols to form alkyl esters. This result is quite surprising because these reactions usually occur when the reaction is performed in the presence of an acid catalyst (i.e., H_2SO_4, and HCl) at reaction temperatures between 40°C and 80°C, as used in the biodiesel production to reduce free fatty acid content [4].

Based on the results discussed above, ozonolysis of non-edible oils or used cooking oils mixed with alcohols might offer a new alternative technique for biodiesel production because non-edible oils or used cooking oils contain a substantial amount of FFAs that react with an alkaline catalyst (i.e., NaOH) to form soaps, resulting in difficult separation processes and decreased conversion rates [4, 5, 38, 39].

There are many advantages to ozonolysis of used cooking oils or non-edible oils mixed with alcohols in the pre-treatment process for biodiesel production. For example, a substantial amount of NN might be formed if OL is the major species of free fatty acid. The NN can be simply separated due to its lowest boiling point. The reactions take place at atmospheric pressure and room temperature and without the use of acid catalysts, resulting in reductions in the use of energy, waste-water treatment, and acid-resistant materials in the piping system. Moreover, the alkyl esters of OcA, NA, AA, and OA can be separated for sale as valuable products and can be directly blended with long-chain alkyl esters to reduce the viscosity of biodiesel.

As also shown in Figure 5A through Figure 5E, methanol is a suitable protic solvent for mixing with OL to increase productivity because the highest concentration of NN is observed. Several advantages can be gained from using methanol. The first advantage is that methanol loss as a result of oxidation by ozone is quite low compared with other alcohols because of methanol's lesser reactivity with ozone.

The second reason is that the diffusion coefficient and the Henry's Law constant for OL mixed with methanol are higher than those of the other mixtures, thus resulting in faster formation of NN. The last reason is that the viscosity of OL mixed with methanol is lower than that of the other mixtures, leading to the formation of smaller bubbles (increase in the specific interfacial area). Therefore, methanol is the selected protic solvent used in this study. However, the only disadvantage to use of methanol is its low boiling point because substantial amounts of methanol might evaporate during ozonolysis.

As discussed, methanol is the selected protic solvent used in this study. Therefore, several different molar ratios were investigated, i.e., 0.5:1.0, 0.75:1.0, 1.0:1.0, 1.5: 1.0, and 2.0:1.0, to find the optimum molar ratio between methanol and OL in terms of NN formation. As shown in Figure 6, the concentration of NN increases dramatically until the molar ratio is equal to 1.0:1.0 and subsequently increases slightly until the molar ratio is equal to 2.0:1.0. Theoretically, the concentration of NN should increase slightly as a result of steady increase in the Henry's Law constant, diffusion coefficient, and specific interfacial area. The reason for the sharp increase of NN at low molar ratio is that all methanol molecules might react with the ozonolysis Criegee Intermediates (CIs) or other carboxylic acids to form methyl esters. Thus, in the absence of methanol, the fluid viscosity increases dramatically because of the formation of higher molecular weight products. The increase of fluid viscosity results in decreases in the specific interfacial area, Henry's Law constant and diffusion coefficient, which all affect the formation of NN.

At a molar ratio of methanol that exceeds 1:1, an amount of methanol molecules still remain in the reactor, leading to slight decreases of the specific interfacial area, Henry's Law constant and diffusion coefficient and a slight increase of NN. Therefore, the optimum molar ratio for methanol and OL in this thesis is 1.0:1.0. This molar ratio is also used to study the different reaction temperatures. It should be noted that an excess molar ratio might be required for commercial production because a small amount of ozone is fed through the reactor in this study, which results in an amount of remaining methanol in the reactor.

In considering the effect of methanol on the formation of NN, the formation of NN increases by 45% when methanol (1:1) is added over ozonolysis with OL and no methanol [40]. However, the increase of NN might be due to the increase of the specific interfacial area, the Henry's law constant, and the diffusion coefficient. This result proves that no reactivity between CIs and NN occurs because all of the CIs react with methanol to form DM-AA and M-NA.

As discussed, ozonolysis of OL mixed with methanol at a molar ratio of 1:1 is the optimum point, and thus, this ratio was used for study at 40°C and 60°C. As illustrated in Figure 7, the concentration of OL decreases with increasing reaction time, but oleic acid methyl ester (M-OL) increases at all reaction temperatures. Although the experiment was conducted for 32 hours, a small amount of M-OL is detected at a reaction temperature of 20°C, as shown in Figure 7A, because the reaction rates the esterification reaction and ozonolysis oxidation reaction are possibly the same at low temperature, resulting in the simultaneous formation of M-OL and any short-chain products.

At a reaction temperature of 40°C, a larger amount of M-OL is observed compared with that at a reaction temperature of 20°C, as shown in Figure 7B and Figure 7C. In addition, a small amount of OL is observed after 8 hours of ozonolysis at 60°C, whereas a large amount of M-OL is observed, which means that most of the OL is converted to M-OL before conversion to NN and short-chain products.

However, it is interesting to note that M-OL still increases with increasing reaction time, as shown in Figure 7D through Figure 7G. Normally, this amount should theoretically decrease because M-OL must be oxidised by ozone at the double bond position to form the products by following the reaction pathway shown in Pfrang et al.[41]. According to these results, certain unknown higher molecular weight products might be formed that cannot be detected by the GC-MS; these unknown products are formed during ozonolysis and might decompose to form M-OL. Moreover, addition of methanol can convert most of the saturated free fatty acids to methyl esters because no peaks of saturated free fatty acids, i.e., OA, PA, and HA, are observed in Figure 7.

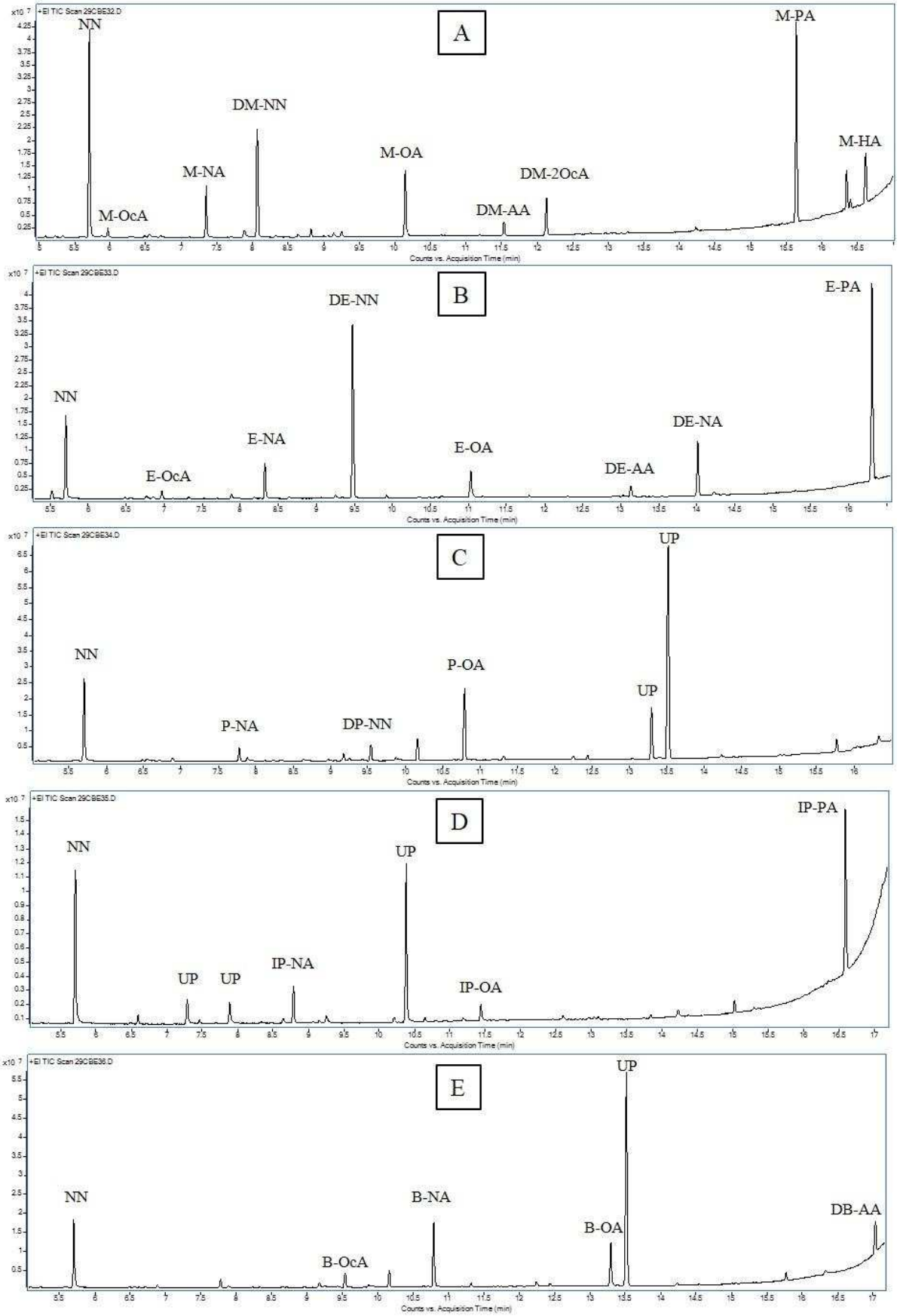

Figure 5 Ozonolysis of OL with alcohols (with 1:1 of molar ratio) at 20oC, 32 hrs; Methanol (A), Ethanol (B), n-propanol (C), iso-propanol (D), and n-butanol (E)

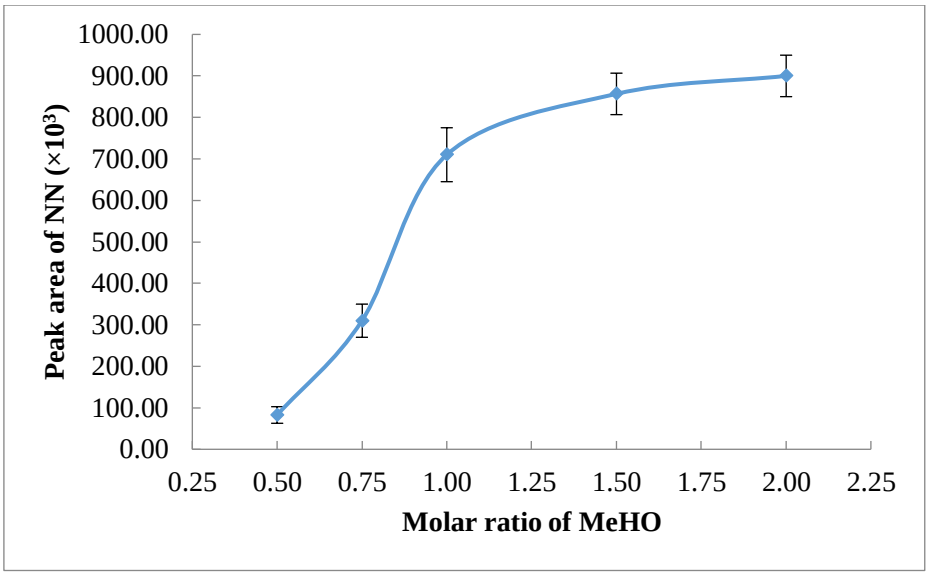

Figure 6 Optimum molar ratio of methanol to OL for 1-nonanal production.

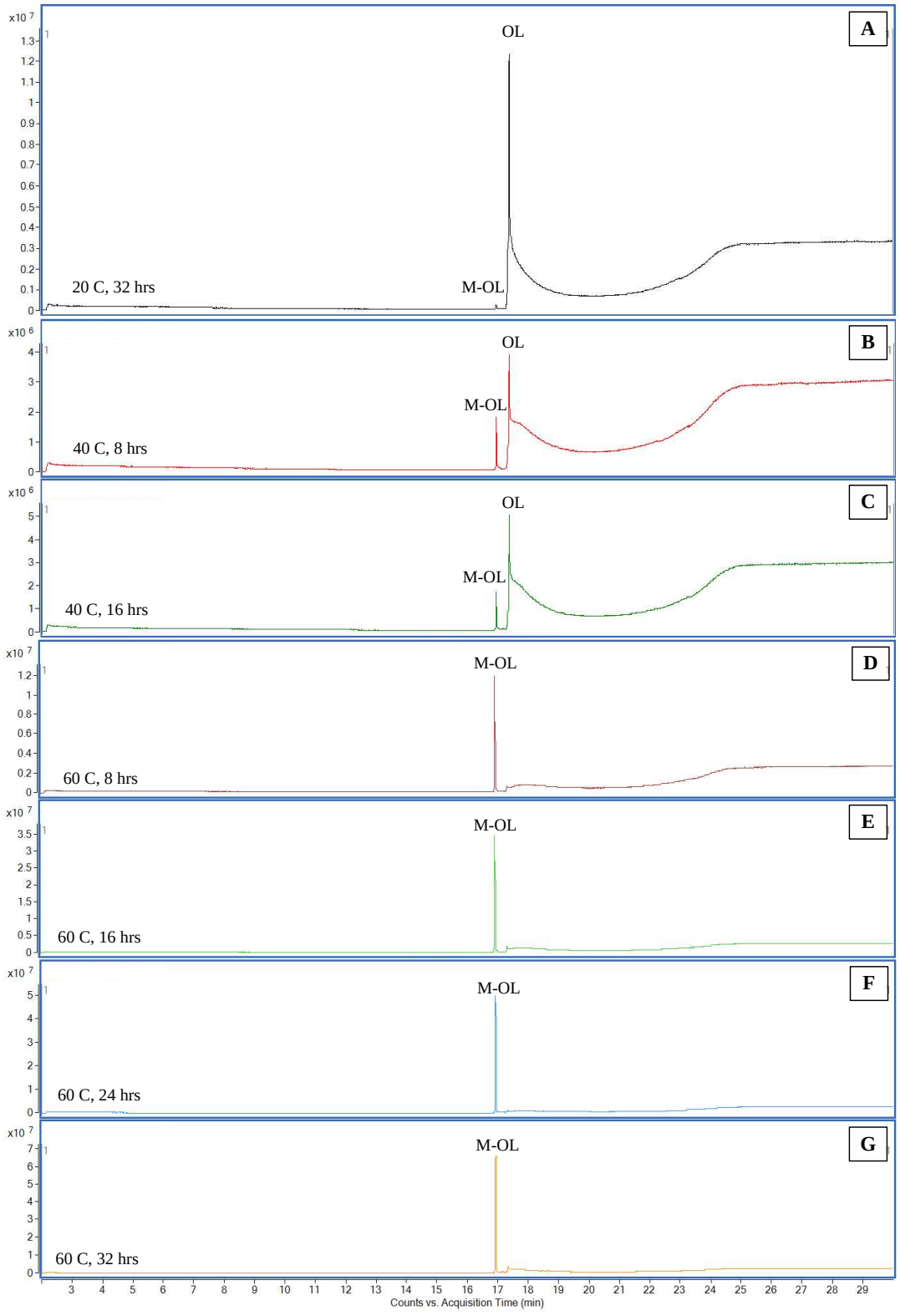

Figure 7 Ozonolysis of OL with methanol (1:1) at different reaction times and temperatures

III. 3 Ozonolysis of used cooking oil

III. 3.1 ASTM D974

Ozonolysis of used cooking oil with 20% FFAs at 20°C, 40°C, and 60°C is shown in Figure 8. Overall, the acid numbers decrease by 25% after 36 hours of ozonolysis. The decrease in the acid numbers relates

directly to the reaction temperatures. The lowest value of acid number is observed in high temperature ozonolysis, whereas these numbers are slightly higher for low temperature ozonolysis. The value of acid number decreases dramatically during the first 12 hours and eventually plateaus.
Because of the low FFAs content in olive oil used in this study [42], it can be assumed that all FFAs in the mixtures before ozonolysis are a combination of OL, PA, SA, and MA. As listed in Table 2, the percentage of saturated FFAs and unsaturated FFAs in the mixtures are 24.8% (PA, SA, and MA) and 75.2 % (OL), respectively.

Based on the experimental results from ozonolysis of OL and methanol solutions, the loss of olive oil in the mixtures during ozonolysis must be higher than that of OL for two reasons: (i) a much higher (~500 times) reaction rate constant of olive oil ozonolysis than that of OL ozonolysis and (ii) a substantial amount of olive oil present in the mixtures. It might be assumed that most of the ozone reacts with olive oil to form NN and M-NA. If the reaction follows this assumption, the reduction of FFAs is only due to esterification of both saturated and unsaturated FFAs. For the worse case, however, if OL reacts with most of the ozone, its concentration will be reduced by 10% (0.01467 mole, 4.63 mL or 4.14 g) over 36 hours of ozonolysis, which means that the acid number must be reduced by direct ozonolysis from 43.63 mg of KOH/g to 40.20 mg of KOH/g or a 7.5% reduction. Therefore, this result can confirm that FFAs are converted to methyl esters via esterification.

Jatropha oil with high FFAs content was recently employed for biodiesel production over carbonaceous magnetic solid catalyst [43]. The acid numbers decrease by 95.8% after reaction with fresh catalyst for 3 hours. However, the reaction temperature, catalyst dosage, and methanol/oil molar ratio are slightly high and the stability of such catalyst still needs improvement for catalyst cycles. These drawbacks are overcome by this novel microbubble process.

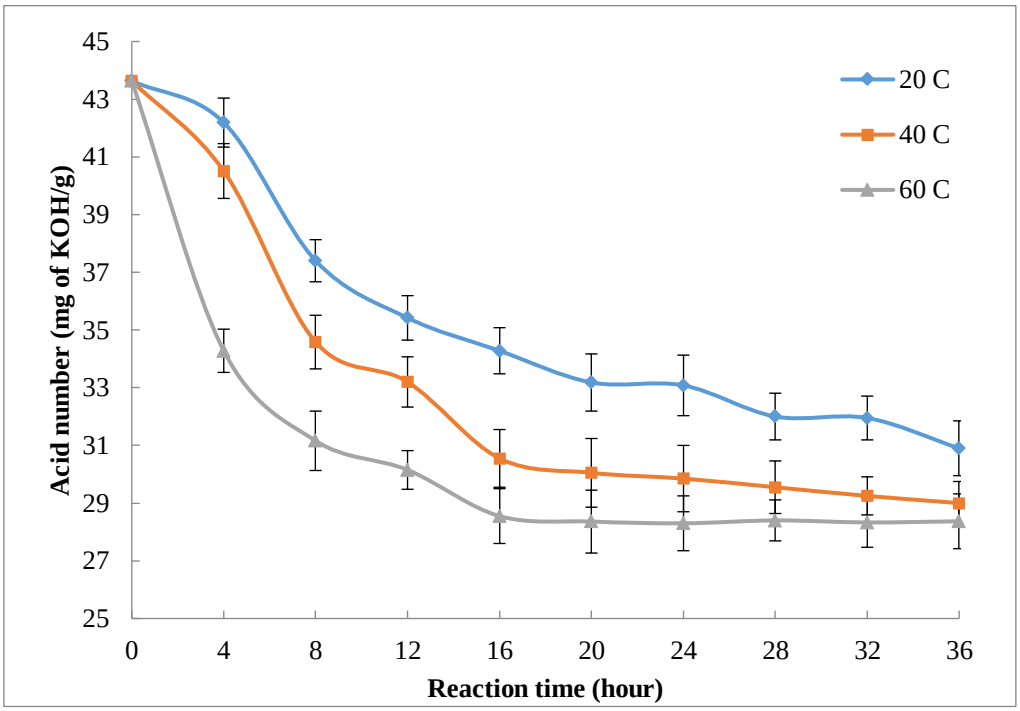

Figure 8 Ozonolysis of used cooking oil at 20% FFAs.

III.3.2 GC-MS
Figure 9 shows the chromatogram of 20% FFAs ozonolysis of at 20°C, 40°C, and 60°C for 32 hours. At 20°C, NN is observed as the major short-chain product, as shown in Figure 9A, whereas M-OL and M-PA are considered to be the major long-chain products. Although M-PA and M-OL are detected, an amount of PA and OL still remains in the system, which is similar to OL ozonolysis in that certain of the carboxylic acids convert to methyl ester in the presence of methanol. In case of ozonolysis at 40°C,

as shown in Figure 9B, the amount of OL and PA decreases slightly, resulting in a slight increase of NN, M-PA, and M-OL. The increase of NN and decrease of OL are due to the increase of the Henry's Law constant, diffusion coefficient, and specific interfacial area at higher temperatures, as discussed in Section III.2. For ozonolysis at 60°C, as shown in Figure 9C, a greater amount of NN, M-PA, and M-OL is observed compared with that of 20°C and 40°C ozonolysis, whereas no peak of PA was detected after 16 hours of ozonolysis. Moreover, although both SA and MA were added into the mixtures, no peaks of these compounds or their relative products, i.e., M-SA and M-MA, were observed because the concentration of the samples injected into the GC-MS is quite low. However, it might be assumed that the reactivities of both SA and MA are similar to that of PA.

In addition to the observation from the chromatograms, the mole balances of PA and M-PA were examined. Although no peak for PA was observed after 16 hours of 60°C ozonolysis, the peak of M-PA still increases up to 20 hours, which means that PA is not simultaneously converted to M-PA; nevertheless, it is converted to unknown species. Such species subsequently decompose to M-PA. However, this result proves that PA is completely converted to M-PA within 20 hours of ozonolysis at 60°C.

Similar to high temperature ozonolysis, most PA is converted to unknown species in low temperature ozonolysis. A difference is that a small amount of unknown species decompose to M-PA. In the case of 20°C and 40°C ozonolysis, for example, the loss of PA is approximately 100% over 32 hours, whereas the formations of M-PA are 16.38% and 35.28%, respectively, which means that the formation of M-PA from unknown species is a function of temperature. In other words, the decomposition rate appears to behave in an Arrhenius manner.

Considering the mole balances of OL and M-OL, the results show that OL is converted to M-OL by 19.46% and 43.79% at 20°C and at 40°C, respectively. The highest conversion of OL to form M-OL is found at 60°C by 91.16%, which means that only OL at 8.84% remains in the system after 32 hours because all of the saturated fatty acids transform to methyl esters, as described previously. Based on the results provided by GC-MS, the percentage of FFAs must be less than 1.33%. This result proves that ozonolysis of used cooking oil is a suitable technique for reduction of free fatty acid content prior to use in biodiesel production.

It is surprising that the results provided by GC-MS are not in good agreement with those provided by ASTM D974. One assumption is that the ASTM D974 technique might have interfered with certain products from ozonolysis of OL, as described in Section III.2. This hypothesis is supported by the change in acid number with reaction time, which decreases sharply at the beginning of ozonolysis and subsequently plateaus. The reason for this observation is that the reaction rate of esterification is higher than that of ozonolysis, resulting in a substantial loss of FFAs. After most of the FFAs are converted to methyl esters, the remaining OL and olive oil still react with ozone to form NN and other products. The loss of OL and the formation of such products are the same, leading to the constant acid numbers. Another supporting piece of evidence is that identical features of the reduction in acid numbers are observed at all different percentages of FFAs. However, further study of the ozonolysis products that affect the determination of acid number is necessary.

III. 4 Discussion of support for the hypothesis

From the two experimental studies conducted here, it is clear that at low liquid temperatures (20°C), ozonolysis and the formation of ozonolysis products, chiefly 1-nonanal, is favoured by injection of room temperature bubbles. At the highest temperature studied, liquid temperature 60°C, 91.2% of the yield of oleic acid is methyl ester (M-OL) according to the GC analysis. Our hypothesis suggested by this motivation is that ozone-rich bubbles injected into methanol-FFA mixtures (no acid or alkaline catalyst present) will be driven towards completion of esterification by the water removal mechanism, but catalysed by free radical chain reaction. Clearly, at the higher liquid temperature, this hypothesis

is supported, and the direction of travel is clear – higher liquid temperature should increase the yield of methyl esters.

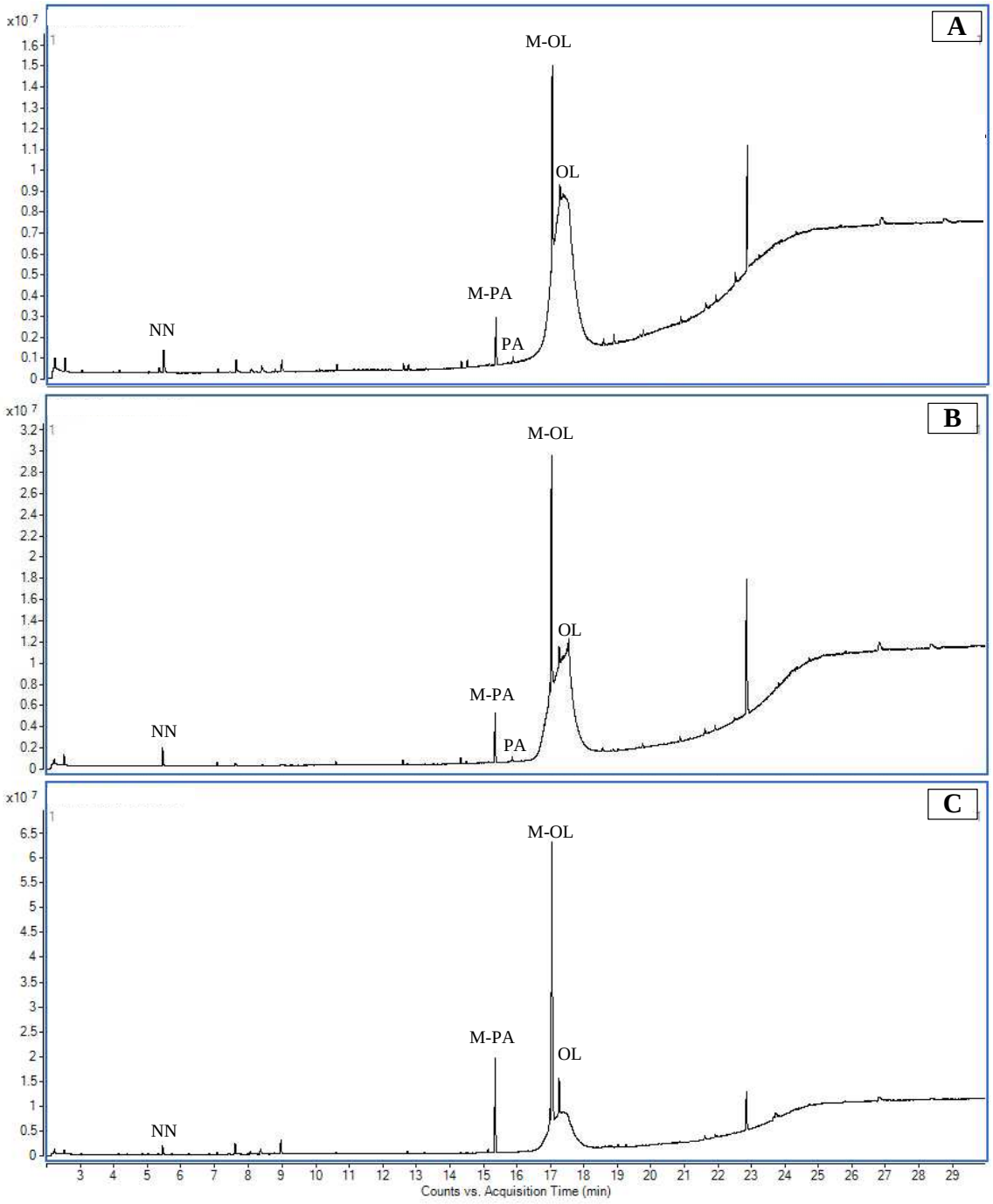

Figure 9 Chromatogram of ozonolysis of used cooking oil at 20% FFAs for 32 hrs: A = 20°C, B = 40°C, and C = 60°C

The temperature dependence is not unexpected. The saturation pressure of water vapour increases dramatically from 20°C to 60°C so that the chemical thermodynamic driver for water removal increase too. Since esterification is an equilibrium reaction that only slightly favors the products, the additional Gibbs free energy release on water vaporisation helps move the reaction towards products. Less obvious is the latent heat of vaporisation, which must be extracted from the system. Because the heating mantle maintains the temperature of the reaction mixture, it is not clear that the latent heat is more

readily available at the higher liquid temperature, but this feature must also favour esterification product formation.

We stated that ozone is a free radical initiator, but actually it is possible to tune an in situ ozone plasma microreactor [24] so that oxygen singlet radicals are preferentially produced by selection of the residence time, and injected directly into the bubble. In the presence of water, oxygen radicals form hydroxyl radicals, but either radical species will form water in the presence of methanol my scavenging the labile hydrogen from the alcohol group, forming the methoxy radical. This part of the hypothesis could not be tested with the "off the shelf" Dryden Aqua ozone generator, as the tuning of the residence time in the plasma reactor was unexplored. The ozone formation kinetics are not controllable to the user of this ozone generator. However, the formation of the oxygen singlet radical is controllable using the plasma microreactor to microbubble generator of [22].

It should also be noted that hot microbubbles were not used in this experimental campaign, which also dramatically increase the vaporisation rate if the contact time is optimised to about a millisecond [19]. Increasing the water removal driving force and forming oxygen radicals rather than ozone at the microbubble interface should enhance the preference for esterification over ozonolysis with unsaturated fatty acids (and triglycerides). For saturated fatty acids, there are no Criegee intermediates to compete with esterification. In this study, we used "simulated used cooking oil", but anecdotal evidence in actual used cooking oil is that the free fatty acid content is much higher than the 20% employed here. Yet all saturated free fatty acids were observed to form methyl esters completely.

III.4 Implications of the current study for esterification of lipids for sustainable biochemicals and fuels.

This is a laboratory based study using readily available "off-the-shelf" equipment (see Figure 3), where the key aspects for industrial scale up have not been designed to be "fit for purpose" – microbubble injection and ozone generation. It is aimed at proof of concept in the lab – NASA technology readiness level (TRL) 3 – rather than the "valley of death" TRL 4-6, which would be large lab that simulates with a scale model the eventual industrial implementation, and pilot scale and pilot plant operations, from which the essential operating parameters and rates are learnt for full industrial scale implementation. It is not possible to conduct a full technical economic analysis from "proof of concept" in the lab, particularly because rates are the central piece of information needed for scale up. Rates can be assessed from TRL 4 (large lab simulating the industrial implementation), but not from lab bench optimisation. Central to the rate estimation is delivery of microbubbles in the industrial configuration, which is likely to be similar to microbubble distillation [17] with a thin layer for the reactor. For separation only, bioethanol removal is highly non-equilibrium [19] using that configuration, which is being built at pilot plant scale currently for integrated reaction and separation.

The key learnings from this work so far is that stoichiometric methanol achieves completion of reaction with ozone-rich microbubbles as the catalyst, which removes the need for downstream separations of either acid or alkaline catalyst, water, and unreacted methanol – all the traditional separation processes for the esterification product stream. For design purposes, the "back of the envelope" chemical engineer's cost estimates are that the capital cost of a plant is proportional to the volume of the unit operations. Conventionally, excess alcohol at the level of 12-fold can be used to force the esterification closer to completion. Recalling that Talebian-Kiakalaieh et al. [4] achieved less than 90% conversion with 70-fold excess methanol reinforces that conventional acid esterification requires a recycle of unspent methanol and downstream separation of unreacted acid catalyst. These two separation steps require vessels of similar volume of the esterifier. With stoichiometric methanol, the likelihood of a small esterifier volume is very high – at least half the size. Removing the need for two downstream separators similarly reduces volumes of unit operations. The above argument would support roughly $1/6^{th}$ of the overall reactor and separator volume of the conventional acid esterifier unit. A second chemical engineers "rule of thumb" for superficial estimation of flowsheet processing costs is that the

utilities cost is proportional to the volume of the unit operations. Hence $1/6^{th}$ reduction in energy use would be the expected "ballpark".

Of course, a thorough technical economic analysis cannot be conducted at this stage, but the crucial issue that needs to be explored is the separation of co-product 1-nonanal, which is far more valuable than biodiesel. An open question that cannot be addressed at this stage is whether the organic mixture produced meets biodiesel standards. Until optimisation studies are conducted for TRL 4, it is not really a sensible question, nor necessarily important at all. In the spirit of the biorefinery, looking for sustainably produced, valuable co-products, is essential to the profitability of the processing of lipids to biochemicals and biofuels. Indeed, it may be more economic to produce valuable esters and aldehydes from this process than biodiesel.

IV. Summary and Conclusions

Ozonolysis of OL was evaluated at different operating temperatures with and without protic solvents (alcohols). In the case of ozonolysis of OL without alcohols, two products (i.e., NN and OA) are observed at 20°C with 93.5±3.4% yield. Additional products (the unidentified species) are also found at both 40°C and 60°C. The unidentified species are generated from decomposition of higher molecular weight species that are formed by the secondary reaction between the Criegee intermediates and oleic acid.

In the case of ozonolysis of OL with alcohols, a greater 1-nonanol content is observed compared with that of the system without alcohols. The increase of 1-nonanol is not influenced by the alcohols or by the increases in the Henry's Law constant, diffusion coefficient, and specific interfacial area. Carboxylic acids and Criegee intermediates formed during ozonolysis are converted to alkyl esters depending on the molecular structure of the alcohols. To increase the productivity of 1-nonanol, methanol is a suitable protic solvent because of its physical properties. The optimum molar ratio between methanol and OL is 1:1. At low temperatures, the reaction rates of OL ozonolysis and OL esterification are identical, whereas at high temperatures, the reaction rate of OL esterification is much higher.

Ozonolysis of used cooking oils at 20% FFAs content was performed at various temperatures. Two techniques were employed to characterise the FFAs content, i.e., ASTM D974 and GC-MS. Using the ASTM D974 technique, the acid numbers decrease dramatically by approximately 25% and subsequently plateau. Similar features of the reduction in acid numbers are observed at all different percentages of FFAs. The lowest values of acid numbers are found in 60°C ozonolysis. Using GC-MS, all of the saturated FFAs, i.e., PA, SA, and MA, convert to methyl esters within 20 hours of 60°C ozonolysis, whereas a small amount remain at lower temperatures. Moreover, after 32 hours of 20% FFAs ozonolysis at 60°C, the conversion of OL is found to be 91.16%, indicating that the FFAs content in used cooking oil is less than 1.33%. This observation confirms that ozonolysis of used cooking oil is an alternative technique for reduction of free fatty acid content for biodiesel production. The "phantom catalyst" achieved the promise of esterification. Stoichiometric amounts of methanol used strongly suggest that the free radical mechanism with water removal does not need the Le Chatelier's push of excess methanol.

Acknowledgments

WZ would like to thank the Engineering and Physical Sciences Research Council for support from grants EP/I027858/1 and EP/I019790/1. WZ thanks Pratik Desai, Hemaka Bandulasena, Jaime Lozano-Parada and David Blythe for helpful discussions. RK was supported by The Royal Thai Government scholarship for his doctoral studies.

References

[1] D. T. Tran, J. S. Chang, and D. J. Lee, "Recent insights into continuous-flow biodiesel production via catalytic and non-catalytic transesterification processes," Applied Energy, vol. 185, pp. 376-409, Jan 2017.
[2] E. E. Kwon, E. C. Jeon, H. Yi, and S. Kim, "Transforming duck tallow into biodiesel via noncatalytic transesterification," Applied Energy, vol. 116, pp. 20-25, Mar 2014.
[3] S. Lim and K. T. Lee, "Process intensification for biodiesel production from Jatropha curcas L. seeds: Supercritical reactive extraction process parameters study," Applied Energy, vol. 103, pp. 712-720, Mar 2013.
[4] A. Talebian-Kiakalaieh, N. A. S. Amin, and H. Mazaheri, "A review on novel processes of biodiesel production from waste cooking oil," Applied Energy, vol. 104, pp. 683-710, Apr 2013.
[5] A. W. Go, S. Sutanto, L. K. Ong, P. L. Tran-Nguyen, S. Ismadji, and Y. H. Ju, "Developments in in-situ (trans) esterification for biodiesel production: A critical review," Renewable & Sustainable Energy Reviews, vol. 60, pp. 284-305, Jul 2016.
[6] C. D. M. de Araujo, C. C. de Andrade, E. D. E. Silva, and F. A. Dupas, "Biodiesel production from used cooking oil: A review," Renewable & Sustainable Energy Reviews, vol. 27, pp. 445-452, Nov 2013.
[7] A. Sarin, Biodiesel : production and properties. Cambridge: Royal Society of Chemistry, 2012.
[8] E. F. Aransiola, T. V. Ojumu, O. O. Oyekola, T. F. Madzimbamuto, and D. I. O. Ikhu-Omoregbe, "A review of current technology for biodiesel production: State of the art," Biomass & Bioenergy, vol. 61, pp. 276-297, Feb 2014.
[9] M. Chai, Q. S. Tu, M. M. Lu, and Y. J. Yang, "Esterification pretreatment of free fatty acid in biodiesel production, from laboratory to industry," Fuel Processing Technology, vol. 125, pp. 106-113, Sep 2014.
[10] F. Zhang, Z. Fang, and Y. T. Wang, "Biodiesel production direct from high acid value oil with a novel magnetic carbonaceous acid," Applied Energy, vol. 155, pp. 637-647, Oct 2015.
[11] F. A. Dawodu, O. Ayodele, J. Y. Xin, S. J. Zhang, and D. X. Yan, "Effective conversion of non-edible oil with high free fatty acid into biodiesel by sulphonated carbon catalyst," Applied Energy, vol. 114, pp. 819-826, Feb 2014.
[12] B. M. E. Russbueldt and W. F. Hoelderich, "New sulfonic acid ion-exchange resins for the preesterification of different oils and fats with high content of free fatty acids," Applied Catalysis a-General, vol. 362, no. 1-2, pp. 47-57, Jun 30 2009.
[13] A. H. M. Fauzi, N. A. S. Amin, and R. Mat, "Esterification of oleic acid to biodiesel using magnetic ionic liquid: Multi-objective optimization and kinetic study," Applied Energy, vol. 114, pp. 809-818, Feb 2014.
[14] A. M. Doyle, T. M. Albayati, A. S. Abbas, and Z. T. Alismaeel, "Biodiesel production by esterification of oleic acid over zeolite Y prepared from kaolin," Renewable Energy, vol. 97, pp. 19-23, Nov 2016.
[15] S. W. Gong, J. Lu, H. H. Wang, L. J. Liu, and Q. Zhang, "Biodiesel production via esterification of oleic acid catalyzed by picolinic acid modified 12-tungstophosphoric acid," Applied Energy, vol. 134, pp. 283-289, Dec 2014.
[16] Y. Zhang, W. T. Wong, and K. F. Yung, "Biodiesel production via esterification of oleic acid catalyzed by chlorosulfonic acid modified zirconia," Applied Energy, vol. 116, pp. 191-198, Mar 2014.
[17] W. B. Zimmerman, M. K. H. Al-Mashhadani, and H. C. H. Bandulasena, "Evaporation dynamics of microbubbles," Chemical Engineering Science, vol. 101, pp. 865-877, Sep 2013.
[18] N. Abdulrazzaq, B. Al-Sabbagh, J. M. Rees, and W. B. Zimmerman, "Separation of azeotropic mixtures using air microbubbles generated by fluidic oscillation," Aiche Journal, vol. 62, no. 4, pp. 1192-1199, Apr 2016.
[19] N. N. Abdulrazzaq, B. H. Al-Sabbagh, J. M. Rees, and W. B. Zimmerman, "Purification of Bioethanol Using Microbubbles Generated by Fluidic Oscillation: A Dynamical Evaporation Model," Industrial & Engineering Chemistry Research, vol. 55, no. 50, pp. 12909-12918, Dec 2016.

[20] G. Knothe, J. H. Van Gerpen, and J. Krahl, The biodiesel handbook, 2nd ed. ed. Champaign, Ill.: American Oil Chemists' Society, 2009.
[21] J. W. Timberlake and M. L. Hodges, "Substituent effects and free radical stability. The methoxy group," Tetrahedron Letters, vol. 11, no. 48, pp. 4147-4150, 1970.
[22] W. B. Zimmerman, "Electrochemical microfluidics," Chemical Engineering Science, vol. 66, no. 7, pp. 1412-1425, Apr 2011.
[23] F. Rehman, Y. Liu, and W. B. J. Zimmerman, "The role of chemical kinetics in using O3 generation as proxy for hydrogen production from water vapour plasmolysis," International Journal of Hydrogen Energy, vol. 41, no. 15, pp. 6180-6192, Apr 2016.
[24] J. H. Lozano-Parada and W. B. Zimmerman, "The role of kinetics in the design of plasma microreactors," Chemical Engineering Science, vol. 65, no. 17, pp. 4925-4930, Sep 2010.
[25] W. S. Abdul-Majeed, G. S. Aal-Thani, and J. N. Al-Sabahi, "Application of Flying Jet Plasma for Production of Biodiesel Fuel from Wasted Vegetable Oil," Plasma Chemistry and Plasma Processing, vol. 36, no. 6, pp. 1517-1531, Nov 2016.
[26] R. Criegee, "Mechanism of ozonolysis," Angewandte Chemie-International Edition in English, vol. 14, no. 11, pp. 745-752, 1975.
[27] M. H. Tavassoli-Kafrani, P. Foley, E. Kharraz, and J. M. Curtis, "Quantification of Nonanal and Oleic Acid Formed During the Ozonolysis of Vegetable Oil Free Fatty Acids or Fatty Acid Methyl Esters," Journal of the American Oil Chemists Society, vol. 93, no. 3, pp. 303-310, Mar 2016.
[28] J. D. Hearn, A. J. Lovett, and G. D. Smith, "Ozonolysis of oleic acid particles: evidence for a surface reaction and secondary reactions involving Criegee intermediates," Physical Chemistry Chemical Physics, vol. 7, no. 3, pp. 501-511, 2005.
[29] G. F. Hirata, C. R. A. Abreu, L. C. B. A. Bessa, M. C. Ferreira, E. A. C. Batista, and A. J. A. Meirelles, "Liquid-liquid equilibrium of fatty systems: A new approach for adjusting UNIFAC interaction parameters," Fluid Phase Equilibria, vol. 360, pp. 379-391, Dec 25 2013.
[30] W. B. Zimmerman, B. N. Hewakandamby, V. Tesar, H. C. H. Bandulasena, and O. A. Omotowa, "On the design and simulation of an airlift loop bioreactor with microbubble generation by fluidic oscillation," Food and Bioproducts Processing, vol. 87, no. C3, pp. 215-227, Sep 2009.
[31] D. Gerlach, N. Alleborn, V. Buwa, and E. Durst, "Numerical simulation of periodic bubble formation at a submerged orifice with constant gas flow rate," Chemical Engineering Science, vol. 62, no. 7, pp. 2109-2125, Apr 2007.
[32] D. Ma, M. Liu, Y. Zu, and C. Tang, "Two-dimensional volume of fluid simulation studies on single bubble formation and dynamics in bubble columns," Chemical Engineering Science, vol. 72, pp. 61-77, Apr 16 2012.
[33] D. J. Wesley, S. A. Brittle, and D. T. W. Toolan, "Development of an optical microscopy system for automated bubble cloud analysis," Applied Optics, vol. 55, no. 22, pp. 6102-6107, Aug 2016.
[34] S. Garcia-Salas, M. E. R. P. Alfaro, R. M. Porter, and F. Thalasso, "Measurement of local specific interfacial area in bubble columns via a non-isokinetic withdrawal method coupled to electro-optical detector," Chemical Engineering Science, vol. 63, no. 4, pp. 1029-1038, Feb 2008.
[35] J. Hanotu, H. C. H. Bandulasena, and W. B. Zimmerman, "Microflotation performance for algal separation," Biotechnology and Bioengineering, vol. 109, no. 7, pp. 1663-1673, Jul 2012.
[36] W. B. Zimmerman, V. Tesar, and H. C. H. Bandulasena, "Towards energy efficient nanobubble generation with fluidic oscillation," Current Opinion in Colloid & Interface Science, vol. 16, no. 4, pp. 350-356, Aug 2011.
[37] W. J. Waddell, S. P. Cohen, J. V. Feron, and I. J. Goodman, "Flavoring substances 23," Institute of Food Technologists, Chicago2007.
[38] M. Balat, "Potential alternatives to edible oils for biodiesel production - A review of current work," Energy Conversion and Management, vol. 52, no. 2, pp. 1479-1492, Feb 2011.

[39] U. Biermann, U. Bornscheuer, M. A. R. Meier, J. O. Metzger, and H. J. Schaefer, "Oils and Fats as Renewable Raw Materials in Chemistry," Angewandte Chemie-International Edition, vol. 50, no. 17, pp. 3854-3871, 2011.
[40] R. Kokoo, "Upgrading of oleic acid, olive oil, and used cooking oil via bubbling ozonolysis," Ph.D., Department of Chemical and Biological Engineering, The University of Sheffield, 2015.
[41] C. Pfrang et al., "Ozonolysis of methyl oleate monolayers at the air-water interface: oxidation kinetics, reaction products and atmospheric implications," Physical Chemistry Chemical Physics, vol. 16, no. 26, pp. 13220-13228, 2014.
[42] C. Peri, The Extra-Virgin Olive Oil Handbook, First ed. John Wiley & Sons, 2014.
[43] Y.-T. Wang, Z. Fang, and X.-X. Yang, "Biodiesel production from high acid value oils with a highly active and stable bifunctional magnetic acid," Applied Energy, vol. 204, no. Supplement C, pp. 702-714, Oct 2017.